hperaza@fis.uc3m.es

1. Introduction

The W7-X stellarator, that started its operation in December of 2015 at the Max-Planck Institute for Plasma Physics in Greifswald [3], has been optimised to provide good MHD equilibrium and stability, improved neoclassical confinement, small bootstrap currents and good fast particle confinement at high beta. However, operating away from this optimised configuration might be interesting in order to further improve certain properties at the expense of others. Among these accessible scenarios, there are many in which self-generated neoclassical bootstrap currents [4, 5, 6] might be significant. The presence of these bootstrap currents could alter some of the good properties of the original design. For instance, the modifications of the rotational transform caused by these bootstrap currents could result in the formation of magnetic islands and stochastic regions inside of the plasma, leading to a reduction of the confining volume and to a decrease of the confined energy. In addition, they might also displace the magnetic island chain that is often positioned at the edge of the plasma to isolate it from the walls and to help to control the particle and energy exhaust towards the divertor plates. If the island chain is moved within the plasma as a result of these modifications, it could reduce the confining volume significantly. If, on the other hand, the island chain is displaced beyond the divertor plates, it would lead to the direct contact of good flux surfaces with the divertor, that would start to function instead as a normal limiter. Many of the well-known advantages of divertor operation in regards to both particle and heat control would thus be lost [7]. Therefore, it is clear that any changes in the size, position and phase of this island chain need to be predicted and counteracted if needed.

Due to their importance for W7-X operation, specially for the foreseen quasi-steady-state operation, a number of procedures for bootstrap current control have been investigated over the years [8, 9, 10, 11]. Two main scenarios are usually considered: a first one at low to mid plasma densities (up to $n_e(0) \leq 1 \times 10^{20} m^{-3}$) in which self-generated bootstrap currents can become significant and where ECCD can be achieved efficiently using the X-2 mode heating scheme of the 140GHz ECRH-system (the X-2 mode cutoff occurs at about $n_e(0) \simeq 1.2 \times 10^{20} m^{-3}$ for typical W7-X parameters); and a second one at higher plasma densities, in which bootstrap currents are smaller (due, among other things, to the larger collisionality) but where X2-ECCD is no longer available and other current drive schemes must be used [8]. In the first type of scenarios, ECCD is considered adequate because the diffusion of the driven current happens on the resistive skin timescale, that is of the order of a few seconds, whilst the total toroidal current evolves on the time scale of the L/R time that is of the order of a few tens of seconds. The analysis of these hypothetical scenarios has been done at W7-X by iterating between an ideal MHD equilibrium code and a transport code. The procedure goes approximately as follows. First, an ideal MHD equilibrium solution is obtained with the VMEC code [12], for the time of interest, throughout the region where the plasma is confined. VMEC is a very fast ideal MHD equilibrium solver, widely used

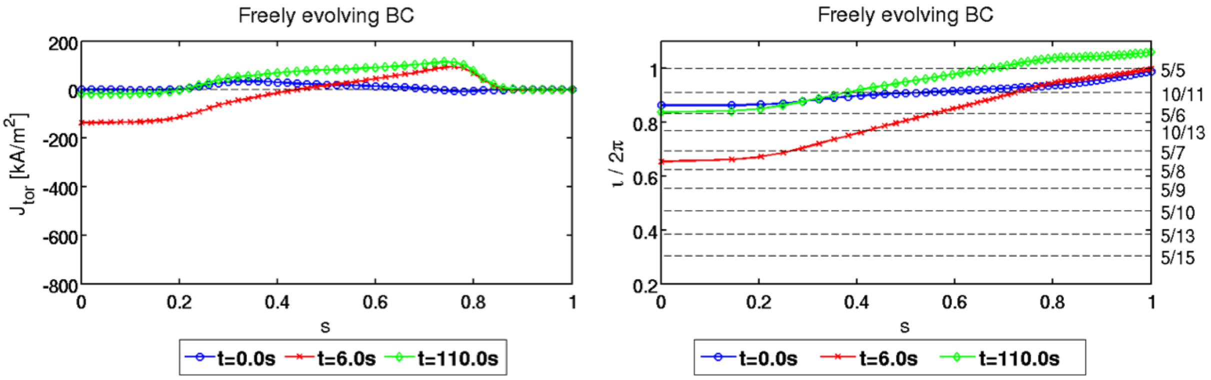
Freely evolving BC
200
0
-200
-400
-600
-800
J_{tor} [kA/m^2]
0
0.2
0.4
0.6
0.8
1
s
t=0.0s
t=6.0s
t=110.0s
Freely evolving BC
1
0.8
0.6
0.4
0.2
ι / 2π
0
0.2
0.4
0.6
0.8
1
s
5/5
10/11
5/6
10/13
5/7
5/8
5/9
5/10
5/13
5/15
t=0.0s
t=6.0s
t=110.0s

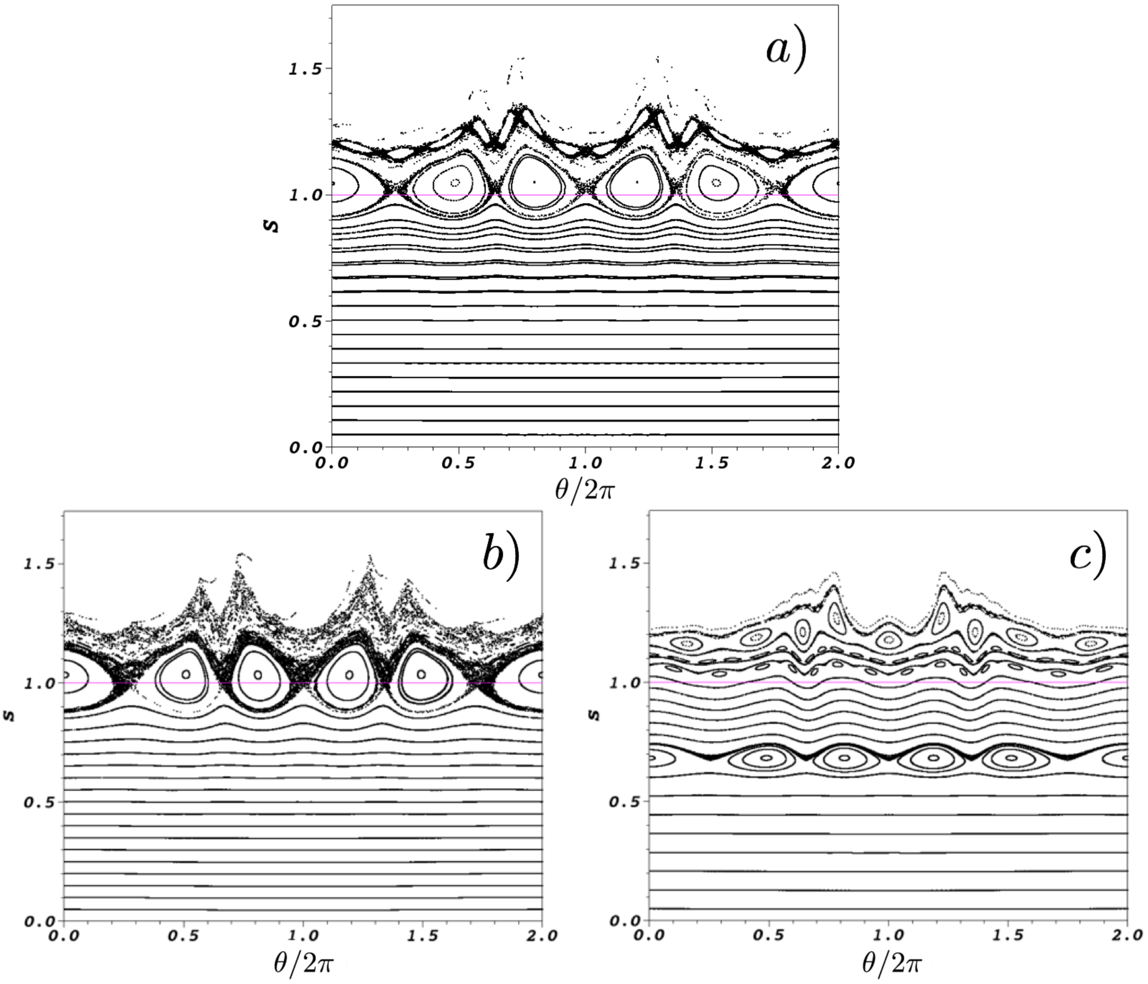
a)
b)
c)
s
θ/2π
0.0
0.5
1.0
1.5
2.0

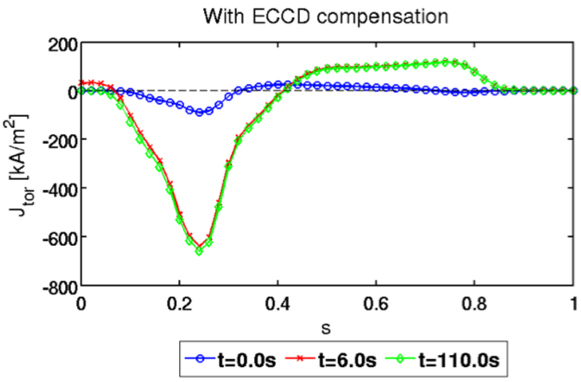
With ECCD compensation

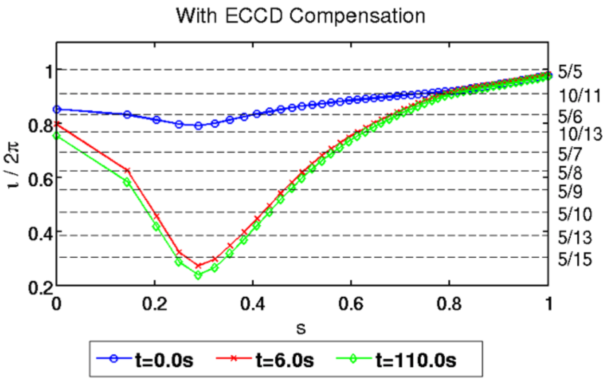
With ECCD Compensation

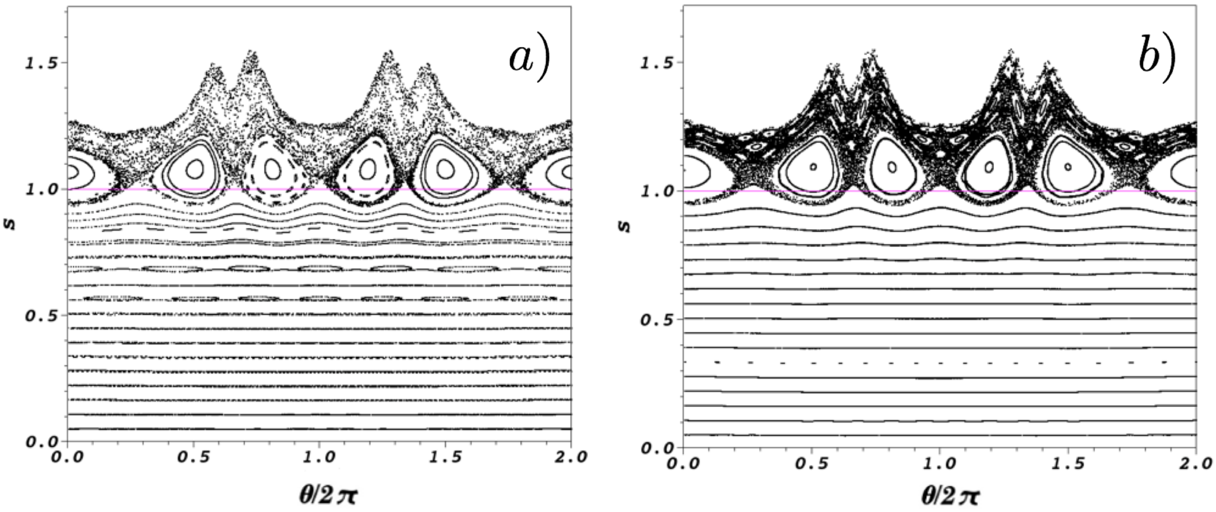
a)
b)
s
θ/2π
0.0
0.5
1.0
1.5
2.0

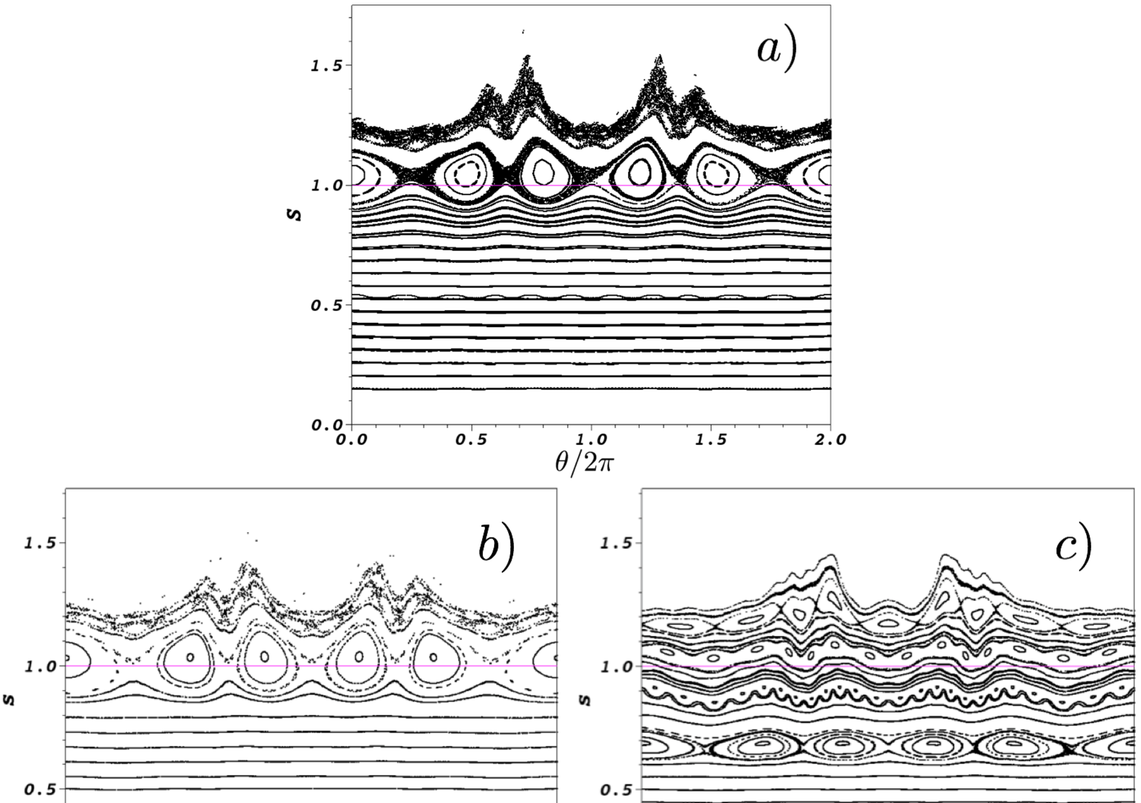
a)
b)
c)
s
θ/2π
0.0
0.5
1.0
1.5
2.0

3.1. *Freely evolving bootstrap current case*

The VMEC runs used to initialize SIESTA in this case have included 49 radial surfaces, 21 poloidal modes and 33 toroidal modes. They are, in fact, the same ones used for the VMEC+EXTENDER procedure described in the previous section. In addition, 34 new radial surfaces have been used to cover the region that extends from the plasma edge to the vacuum vessel. The number of Fourier modes in SIESTA, however, has remained the same. No additional resonant magnetic perturbation has been added during the SIESTA run. Only a finite resistivity has been allowed, for the first few nonlinear iterations, to allow for the diffusion of the current sheets otherwise preventing the formation of magnetic islands. After this initial phase, the resistivity is set to zero so that a convergence to an ideal MHD equilibrium solution can be achieved [1]. Typically, convergence is declared when the normalized residual force squared becomes of the order of $< F^2 > \sim 10^{\ 18} - 10^{\ 20}$. The calculation requires a few hours (typically, from 4 to 6) for each of the times in the scenarios that were examined.

The topology of the magnetic fields obtained by SIESTA for the freely-evolving bootstrap current case are shown in Fig. 5, where Poincaré plots are shown at times $t = 0$, $t = 6$ and $t = 100$ sec. These puncture plots should be compared with those obtained by the VMEC+EXTENDER combo in Fig. 2. The first reassuring observation is that the main features are similar, particularly outside of the plasma (i.e., for $s > 1$). For instance, the 5/5 island chain is found at the plasma edge at $t = 6$ sec, although it is perhaps a bit wider in the SIESTA solution. At $t = 100$ sec, on the other hand, the 5/5 chain has entered the plasma and is located at around $s \sim 0.65 - 0.75$, almost at the same position as in the VMEC+EXTENDER solution. One can also see in both solutions that the 15/14 and 10/9 rationals are present in the region between the plasma and the vacuum vessel for $t = 110$ sec.

The largest differences appear however inside of the plasma where magnetic islands were absent in the VMEC+EXTENDER solution (except for the 5/5 rational at $t = 100$ sec) but, in the SIESTA case, small-width island chains are seen at $s \sim 0.6$ (where the 10/11 rational is located) for $t = 0$ and at $s \sim 0.4$ (where the 10/13 rational sits) for the other two time points. In addition, another island chain appears close to $s \sim 0.2$ (probably, related to the 5/7 rational) at time $t = 110$, together with a small stochastic region at about $s = 0.1$ (this might be related to the closeness of the 5/6 rational to the axis; it is also worth pointing out that the magnetic axis is the position where the solution of SIESTA, as that of VMEC, is less precise). In spite of these differences, the expected impact on confinement seems to be small due to the small width of the islands. This is probably due to the fact that, in this configuration, the magnetic shear is sufficiently small to keep low-order rationals separated and sufficiently large to keep their size small. As a result, the well-known Chirikov's resonance-overlap criterion [29] is not violated and stochastization does not take

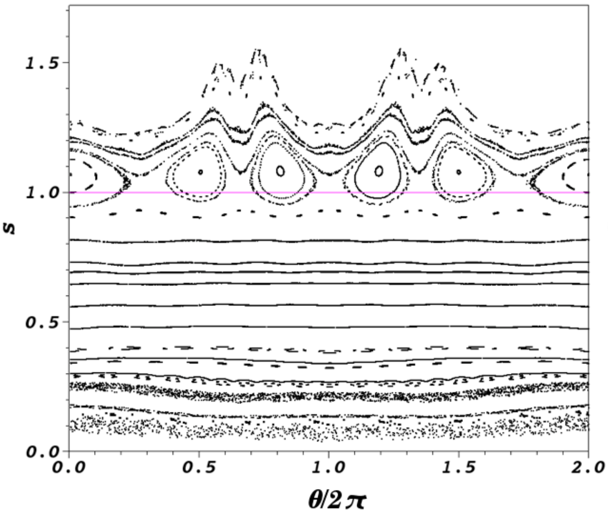

1.5
1.0
0.5
0.0
s
0.0
0.5
1.0
1.5
2.0
θ/2π

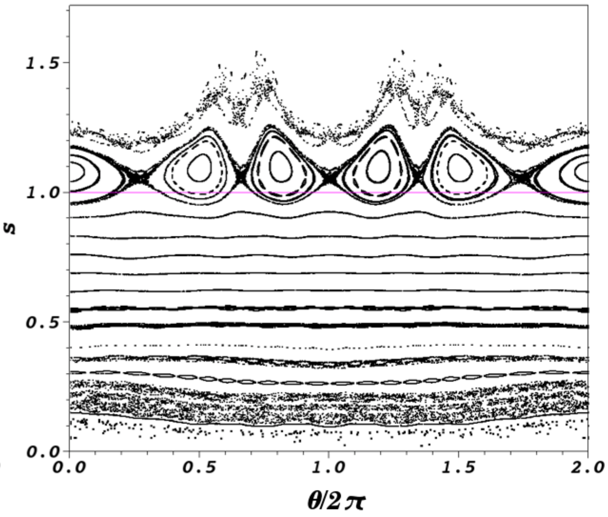

1.5
1.0
0.5
0.0
s
0.0
0.5
1.0
1.5
2.0
θ/2π

SIESTA: A scalable iterative equilibrium solver for toroidal applications

Extension of the SIESTA MHD equilibrium code to free-boundary problems

Confirmation of the topology of the Wendelstein 7-X magnetic field to better than 1:100,000
"Diffusion-electrical phenomena in a plasma confined in a tokamak machine"

Diffusion driven plasma currents and bootstrap tokamak".

On the bootstrap current in stellarators and tokamaks

Effects of divertor geometry on tokamak plasmas

Effects of Net Currents on the Magnetic Configuration of W7-X
Transport modelling of operational scenation in W7-X
Physics in the magnetic configuration space of W7-X

Access to edge scenarios for testing a scraper element in early operation phases of Wendelstein 7-X
Three-dimensional free boundary calculations using a spectral Green's function method
Neoclassical transport simulations for stellarators

Variational bounds for transport coefficients in three-dimensional toroidal plasmas

Large Scale Bayesian Data Analysis for Nuclear Fusion Experiments

PIES free boundary stellarator equilibria with improved initial conditions

Use of the virtual-casing principle in calculating the containing magnetic field in toroidal plasma systems

The virtual-casing principle and Helmholz theorem

Chaos and structures in nonlinear Plasmas

Computation of zero- three dimensional equilibria with magnetic islands

Magnetic islands and singular currents at rational surfaces in three-dimensional magnetohydrodynamic equilibria

Verification of the ideal magnetohydrodynamic response at rational surfaces in the VMEC code

MHD equilibrium of a low-shear helical axis Heliotron.

Computation of multi-region relaxed MHD equilibria

ECRH and ECCD scenarios for W7-X

Ray-tracing code for heating, current drive and diagnostic

Surface current on the plasma-vacuum interface in MHD equilibria

th

Electron cyclotron current drive in the Wendelstein 7-AS stellarator"

A universal instability of many-dimensional oscillator systems

Magnetic reconnection in plasmas

Solution of drift kinetic equation in stellarators and tokamaks with broken symmetry using the code NEO-2

Monte Carlo estimation of neoclassical transport for the TJ-II stellarator

Comparison of particle trajectories and collision operators for collisional transport in nonaxisymmetric plasmas

Resonant magnetic perturbations of edge-plasmas in toroidal confinement devices

First measurements of error fields on W7-X using flux surface mapping